



## N-Benzylimidazole carboxamides as potent, orally active stearoylCoA desaturase-1 inhibitors

Karen A. Atkinson, Elena E. Beretta, Janice A. Brown, Mayda Castrodad, Yue Chen, Judith M. Cosgrove, Ping Du, John Litchfield, Michael Makowski, Kelly Martin, Thomas J. McLellan, Constantin Neagu, David A. Perry, David W. Piotrowski\*, Claire M. Steppan, Richard Trilles

Pfizer Global Research & Development, Groton Laboratories, Pfizer Inc. Groton, CT 06340, USA

### ARTICLE INFO

#### Article history:

Received 28 December 2010

Accepted 25 January 2011

Available online 31 January 2011

#### Keywords:

Stearoyl-CoA desaturase

Obesity

SCD-1

### ABSTRACT

A potent, small molecule inhibitor with a favorable pharmacokinetic profile to allow for sustained SCD inhibition *in vivo* was identified. Starting from a low MW acyl guanidine (**5a**), identified with a RapidFire High-Throughput Mass Spectrometry (RF-MS) assay, iterative library design was used to rapidly probe the amide and tail regions of the molecule. Singleton synthesis was used to probe core changes. Biological evaluation of a SCD inhibitor (**5b**) included *in vitro* potency at SCD-1 and *in vivo* modulation of the plasma desaturation index (DI) in rats on a low essential fatty acid (LEFA) diet. In addition to dose-dependent decrease in DI, effects on rodent ocular tissue were noted. Therefore, in rat, these SCD inhibitors only recapitulate a portion of phenotype exhibited by the SCD-1 knockout mouse.

© 2011 Elsevier Ltd. All rights reserved.

Stearoyl-CoA desaturase (SCD) is an endoplasmic reticulum (ER) enzyme that catalyzes the rate limiting step in the formation of monounsaturated fatty acids. In humans, there is a strong correlation between elevated SCD-1 activity and plasma triglyceride levels and elevated SCD-1 activity in skeletal muscle is positively associated with increased percentage of body weight.<sup>1</sup> Mice that are deficient in SCD-1 have increased energy expenditure, reduced body adiposity, increased insulin sensitivity and are resistant to diet-induced obesity and hepatic steatosis.<sup>2</sup> These observations suggest inhibition of SCD-1 as a potential therapeutic target for the treatment of obesity and metabolic syndrome.<sup>3</sup> Several preclinical SCD-1 inhibitors have been disclosed in the past few years: Abbott (**1**),<sup>4</sup> CVT-12,202 (**2**),<sup>5</sup> MF-152 (**3**),<sup>6</sup> and Pfizer (**4**) (Fig. 1). Previous work with **4** demonstrated *in vivo* modulation of the plasma desaturation index but also degeneration of the harderian and meibomian glands in rodent ocular tissues.<sup>7</sup>

We sought to identify a potent rodent tool compound from an alternative series that, if successful, might also act as a lead for a human agent. Assessment of a compound from a distinct chemical series would allow for discerning mechanism based effects (e.g., SCD-1 inhibition) from potential chemotype toxicity. As such, a desirable compound should possess a favorable pharmacokinetic profile to allow for sustained SCD inhibition *in vivo* and be free from polypharmacology and obvious safety issues (i.e., CYP inhibition, Ames, hERG).

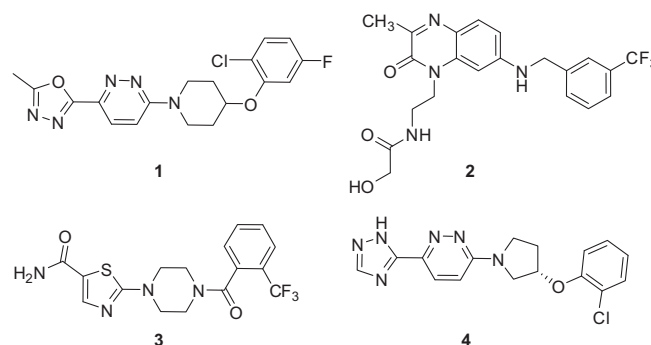


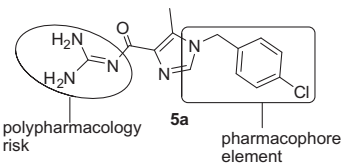
Figure 1. SCD-1 inhibitors.

The corporate compound collection was screened with a RapidFire High-Throughput Mass Spectrometry (RF-MS) assay using rat liver microsomes as the enzyme source. This high throughput mass spectroscopy technique was used to quantitate the formation of deuterated oleoylCoA from deuterated stearoylCoA.<sup>8</sup> Further *in vitro* characterization of the identified hits included screening in orthogonal assay systems that used tritiated stearoylCoA and rat liver microsomes from rats on a low essential fatty acid diet and human liver microsomes as the enzyme sources.<sup>4,9</sup> A reasonably potent, low MW acyl guanidine **5a** was identified but it suffered from moderate permeability and polypharmacology, including hERG inhibition (see Table 1). Based on SCD-1 compounds from the literature we hypothesized that the benzyl group

\* Corresponding author. Tel.: +1 860 686 0271.

E-mail address: [david.w.piotrowski@pfizer.com](mailto:david.w.piotrowski@pfizer.com) (D.W. Piotrowski).

**Table 1**  
Pharmacological, ADME and safety properties of **5a**



<b>5a</b>	
MW 291.7, <i>e</i> Log <i>D</i> 1.2, TPSA 99	
HTMS rSCD-1 IC <sub>50</sub>	68 nM
[ <sup>3</sup> H]-stearylCoA rSCD-1 IC <sub>50</sub>	94 nM
hSCD-1 IC <sub>50</sub>	217 nM
PAMPA <sup>a</sup> (Papp, 10 <sup>-6</sup> cm/s)	2.6
RLM CLint (μL/min/mg)	74.1
HLM CLint (μL/min/mg)	15.5
CEREP/Bioprint™ panel	>15 assays with IC <sub>50</sub> <10 μM
CYP1A2, 2C9, 2D6, 3A4 (pct inh at 3 μM)	<1%
DOF <sup>b</sup> (pct inh at 10 μM)	64%

<sup>a</sup> PAMPA = Parallel artificial membrane permeability assay.

<sup>b</sup> DOF = [<sup>3</sup>H]-dofetilide binding assay.<sup>12a,b</sup>

of the imidazole served as the key pharmacophoric element similar to the *o*- or *m*- (pseudo)halo substituted aryl groups of known SCD-1 matter. We also hypothesized that the acyl guanidine moiety in **5a** contributed to the polypharmacology and hERG liabilities since this functional group is present in drugs known to exert effects on ion channels (e.g., amiloride,<sup>10</sup> zonisamide<sup>11</sup>).

Early on, a small cohort of compounds was tested in both the rat and human enzyme assays. The IC<sub>50</sub> data from these assays were generally within two- to three-fold of each other. We found that replacement of the guanidine moiety of **5a** with an *N*-methylpyrazole **6a** gave a compound that was not only more potent (Table 2) but also more selective as judged by polypharmacology risk with only two assays in the CEREP/Bioprint™ panel with IC<sub>50</sub> <10 μM.

Based on the encouraging data from **6a**, the chemical matter in this series was developed using a combination of parallel synthesis and singleton synthesis. We elected to use the [<sup>3</sup>H]-stearylCoA assay system with rat liver microsomes as the primary assay. Compounds made by library synthesis were first screened in triplicate for percent inhibition at a single 5 μM dose followed by IC<sub>50</sub> determination if warranted.

Iterative library design was used to rapidly probe the tail and amide regions of the molecule. A three-step library procedure, outlined in Scheme 1, was used to probe the tail region. Treatment of **7** with DMF-DMA provided enamine **8**, which was reacted with a wide range of substituted aryl, benzyl and aliphatic amines and saponified to provide imidazole acids **9**. The acids **9** were treated with a narrow range of aminoheterocycles under standard amide coupling conditions to provide imidazole amides **5**. Gram quantities of selected *N*-benzyl imidazole acids **9** and **10**<sup>13</sup> were synthesized as outlined in Schemes 1 and 2. A one-step library protocol was designed to probe variation of the amide substituent. A range of amino heterocycles similar to *N*-methylpyrazole and a diverse set of aliphatic amines were coupled under standard amide bond formation conditions (HATU or HBTU) with **9** or **10** to provide amides **6** and **5**, respectively.

The heterocyclic core determines the position of each substituent and can have strong impact on the physicochemical properties of the final compounds. Such changes were less amenable to variation through parallel chemistry methodology, therefore these changes were probed with singleton synthesis to afford analogs **14**–**17**. Heterocyclic esters, either from commercial sources or synthesized according to Schemes 3 and 4, were alkylated with the appropriate benzyl halide. In some cases, regioisomeric alkylation

products were obtained. These could be separated by standard column chromatography. The esters were saponified to provide the required *N*-benzyl pyrazole and triazole acids **13** as generally depicted in Scheme 5. The acids were then coupled to appropriate heterocyclic amines.

General SAR trends could be gleaned from the tail and amide region libraries. These trends are represented by the selected compounds shown in Table 2. Benzylic tail moieties (**6b**–**f**, **6i**) were highly preferred over phenyl (data not shown) or phenethyl (**6h**) substitution. A single meta substituent, such as Cl or CF<sub>3</sub>, on the pendant benzyl group generally led to more ligand efficient inhibitors. When the core or amide group was less optimal, potency could often be boosted by addition of a para halogen (e.g., **6c**, **6i**, **15**). However, this offered no advantage toward our goal for in vivo activity since the increase in log *P* associated with this change often resulted in lower microsomal stability and lower solubility. In some cases, highly specialized aliphatic groups were also tolerated tail substituents (**6g**). Similar trends were noted for the amide region. Small five-membered aminoheterocycles were highly preferred (e.g., **6b**, **6d**, **6f**). Aliphatic cyclic (data not shown) or acyclic amines (e.g., **6i**) or selected six-membered aminoheterocycles were tolerated but usually resulted in a one to two order of magnitude loss in potency.

Multiple five- and six-membered ring cores, with both *N*-linked and *C*-linked tails, were assessed. For ease of synthesis and best balance of physical properties and ADME characteristics, the imidazole core was preferred (e.g., **6b**). The 1*H*-pyrazole-3-carboxamide **14** and triazole **15** cores were well tolerated, while the 1*H*-pyrazole-4-carboxamide **17** was less potent.

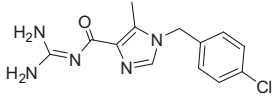
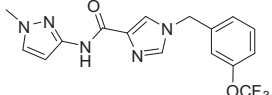
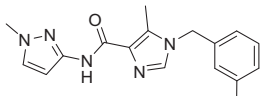
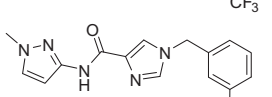
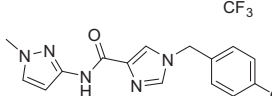
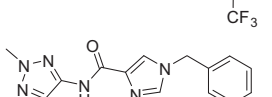
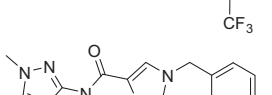
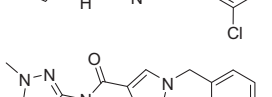
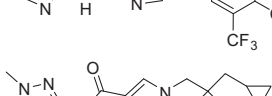
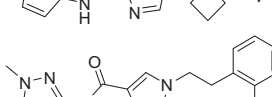
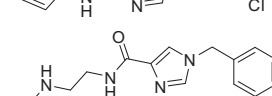
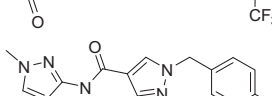
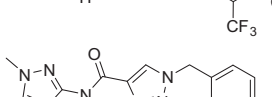
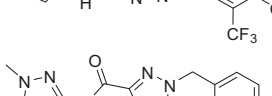
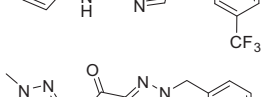
Compounds **5b**, **6b**, **14**, and **15** were selected for further evaluation based upon their promising in vitro profiles. The in vitro human and rat microsomal clearance as well as the in vivo rat pharmacokinetic data are summarized in Table 3. In vitro, all compounds had low to moderate clearance in human liver microsomes (HLM) but were highly variable in rat liver microsomes (RLM). In vivo, compounds **5b** and **17** exhibited moderate clearance, moderate volume of distribution, moderate half life and good bioavailability, while **6b** and **15** had clearances that were significantly higher than rat liver blood flow. The stark contrast in the metabolic fate of **6b** versus **5b** in rats was puzzling. Further assessment of **6b** revealed very low renal and bile excretion as well as good stability in rat plasma. While amide hydrolysis can be offered as a possible explanation, a definitive explanation for the very high rat in vivo clearance for **6b** (and **15**) was not determined. It is notable that both **6b** and **15** were susceptible to degradation in RLM in the absence of co-factors for CYP enzymes (nonmetabolic decline).

Compound **5b** was further assessed in an advanced battery of in vitro assays (Table 4). Of note was the high selectivity over P450 enzymes and selectivity over a wide panel of enzymes, receptors and ion channels. Based on the rSCD-1 potency, low human and rat in vitro CL, moderate in vivo rat CL and a good in vitro safety profile, compound **5b** was selected for further in vivo characterization.

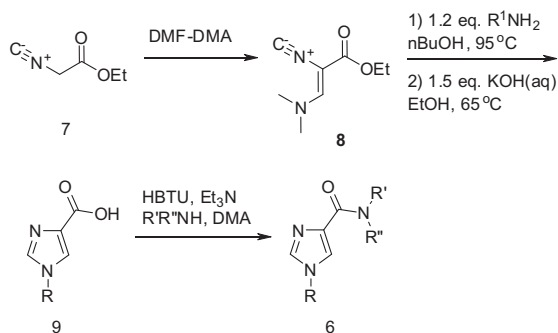
In rodents, it has been demonstrated that short-term feeding of a low-fat, high-carbohydrate diet increases hepatic SCD-1 expression.<sup>14</sup> Thus, an acute rat study, using the desaturation index (DI) as an in vivo biomarker, was used to assess efficacy of **5b**. DI, which correlates with hyperlipidemia,<sup>15</sup> was calculated as ratio of total oleic acid: stearic acid concentrations in plasma. Concentrations of stearic and oleic acid were determined by direct quantitation of extracted stearic and oleic acid from plasma by LC/MS.

Sprague–Dawley rats (*n* = 8 per dose group) were fasted for 20 h, then fed a low essential fatty acid (LEFA) diet<sup>16</sup> for 24 h. The next day, the rats were dosed (po) with **5b** (vehicle 0.5% methylcellulose). Plasma samples were taken three hours post dose. Compound **5b** showed a dose-dependent decrease in DI with a

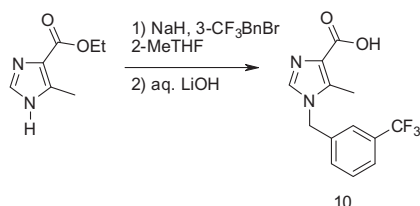
**Table 2**  
Inhibitory properties of selected analogs versus rSCD-1

Compd	Structure	rSCD-1 IC <sub>50</sub> (nM) <sup>a</sup>	hSCD-1 IC <sub>50</sub> (nM) <sup>a</sup>
5a		94	217
6a		32	88
5b		11.7	—
6b		11	—
6c		16	—
6d		25	—
6e		57	—
6f		63	—
6g		101	—
6h		126	—
6i		2750	—
14		63	—
15		33	—
16		113	—
17		2140	—

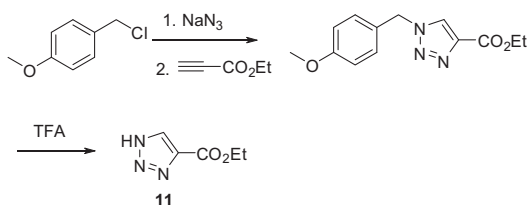
<sup>a</sup> Where available, values are means of two to four experiments.



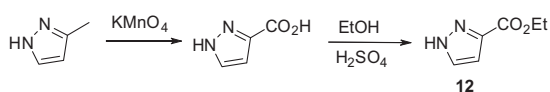
**Scheme 1.** Synthesis of imidazole amides.



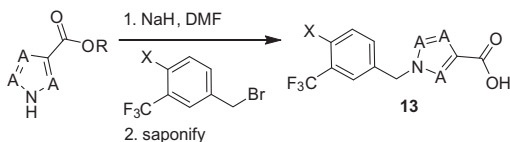
**Scheme 2.** Synthesis of 1-benzyl-5-methylimidazole carboxylic acid.



**Scheme 3.** Synthesis of triazole ester 11.



**Scheme 4.** Synthesis of pyrazole ester 12.



**Scheme 5.** Synthesis of heterocyclic acids 13.

**Table 4**  
Pharmacological, ADME and safety properties of **5b**

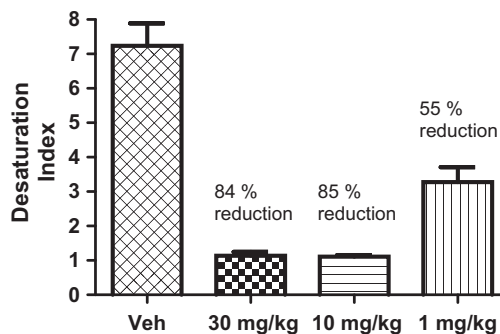
<b>5b</b>	
Rat SCD-1 IC <sub>50</sub>	11.8 ± 1.8 nM
CEREP/Bioprint™ panel (73 assays)	One assay at IC <sub>50</sub> <10 μM
CYP1A2, 2C9, 2C19, 2D6, 3A4	IC <sub>50</sub> >30 μM
hERG patch clamp IC <sub>50</sub>	28.9 μM
Ames	Negative

**Table 5**  
Plasma concentration and DI

Dose (mg/kg)	Total plasma concentration (ng/mL)	Free plasma concentration (nM) <sup>a</sup>	DI	% DI reduction
Veh	—	—	7.24	—
1	56.8	17.6	3.28	55
10	1703	533.5	1.11	85
30	6491	2035	1.14	84

<sup>a</sup> Rat plasma protein binding fu = 0.114, rat IC<sub>50</sub> = 11 nM (3.997 ng/mL).

55% reduction at 1 mg/kg and 85% reduction at the 10 and 30 mg/kg doses (Table 5). The unbound drug plasma concentration was above the *in vitro* rat IC<sub>50</sub> at all doses for the duration of the experiment. Following completion of the experiment, the animals were held for observation. Assessment of eye effects was performed at 27 h post-dose. Mild to moderate effects in ocular tissues (red eyes) were noted in rats from all dosing groups.



In conclusion, acyl guanidine **5a** was identified as a hit using a RapidFire High-Throughput Mass Spectrometry (RF-MS) assay. SCD-1 activity was confirmed in multiple orthogonal assay systems. Iterative library design was used to rapidly probe the amide and tail regions of the molecule and singleton synthesis was used to probe core changes leading to identification of **5b** as an appropriate *in vivo* tool compound. Compound **5b** achieved high exposure *in vivo* to effect dose-dependent modulation of the plasma desaturation index (DI) in rats on a low essential fatty acid (LEFA) diet. However, mild to moderate effects on ocular tissues were noted for all dosing groups. These results, together with other

**Table 3**  
Pharmacokinetic profiles of selected SCD-1 inhibitors

Compd	HLM, CL <sub>int</sub> (μL/min/mg)	RLM, CL <sub>int</sub> (μL/min/mg)	Rat CL (mL/min/kg)	Rat V <sub>ss</sub> (L/kg)	Rat t <sub>1/2</sub> , h (po)	Rat F (%)
<b>5b</b>	<8.0	<18.0	43	4.5	2.3	52
<b>6b</b>	<8.0	— <sup>a</sup>	463	8.1	—	—
<b>14</b>	25.9	72.3	30	0.7	1.3	66
<b>15</b>	<8.0	— <sup>a</sup>	641	10.2	—	—

<sup>a</sup> Nonmetabolic decline.

reports,<sup>4,6,17</sup> suggest effects on eye tissues seen with SCD-1 inhibitors are an on-target rather than chemical series specific side effect. These side effects will need to be overcome if SCD-1 inhibitors are to realize their potential in the treatment of diabetes.

## References and notes

1. (a) Warensjö, E.; Rosell, M.; Hellenius, M.-L.; Vessby, B.; De Faire, U.; Risérus, U. *Lipids Health Dis.* **2009**, *8*, 37; (b) Jeyakumar, S. M.; Lopamudra, P.; Padmini, S.; Balakrishna, N.; Giridharan, N. V.; Vajreswari, A. *Nutr. Metab.* **2009**, *6*, 27.
2. Binczek, E.; Jenke, B.; Holz, B.; Gunter, R. H.; Thevis, M.; Stoffel, W. *Biol. Chem.* **2007**, *388*, 405.
3. Brown, J. M.; Rudel, L. L. *Curr. Opin. Lipidol.* **2010**, *21*, 192.
4. Liu, G.; Lynch, J. K.; Freeman, J.; Liu, B.; Xin, Z.; Zhao, H.; Serby, M. D.; Kym, P. K.; Suhar, T. S.; Smith, H. T.; Cao, N.; Yang, R.; Janis, R. S.; Krauser, J. A.; Cepa, S. P.; Beno, D. W. A.; Sham, H. L.; Collins, C. A.; Surowy, T. K.; Camp, H. S. *J. Med. Chem.* **2007**, *50*, 3086.
5. Koltun, D. O.; Zilbershtein, T. M.; Migulin, V. A.; Vasilevich, N. I.; Parkhill, E. Q.; Glushkov, A. I.; McGregor, M. J.; Brunn, S. A.; Chu, N.; Hao, J.; Mollova, N.; Leung, K.; Chisholm, J. W.; Zablocki, J. *Bioorg. Med. Chem. Lett.* **2009**, *19*, 4070.
6. Li, C. S.; Belair, L.; Guay, J.; Murgasva, R.; Sturkenboom, W.; Ramtohl, Y. K.; Zhang, L.; Huang, Z. *Bioorg. Med. Chem. Lett.* **2009**, *19*, 5214.
7. Beretta, E.; Trebino, C.; Cosgrove, J.; Brown, J.; Martin, K.; Du, P.; Chen, Y.; Bertinato, P.; Cameron, K.; Piotrowski, D.; Marcek, J.; Soulard, P.; Geoghegan, K.; Cornelius, P.; Scott, D.; Chu-Moyer, M.; Swick, A.G.; Stepan, C.M. presented at the Keystone Symposium on Neuronal Mechanisms Controlling Food Intake, Glucose Metabolism and Body Weight, Banff, Alberta, Canada, February, 2008.
8. Soulard, P.; McLaughlin, M.; Stevens, J.; Connolly, B.; Coli, R.; Wang, L.; Moore, J.; Kuo, M.-S. T.; LaMarr, W. A.; Ozbal, C. C.; Bhat, B. G. *Anal. Chim. Acta* **2008**, *627*, 105.
9. Talamo, B. R.; Bloch, K. *Anal. Biochem.* **1969**, *29*, 300.
10. Cuthbert, A. W. *Mol. Pharmacol.* **1976**, *12*, 945.
11. (a) Guzman-Perez, A.; Wester, R. T.; Allen, M. C.; Brown, J. A.; Buchholz, A. R.; Cook, E. R.; Day, W. W.; Hamanaka, E. S.; Kennedy, S. P.; Knight, D. R.; Kowalczyk, P. J.; Marala, R. B.; Mularski, C. J.; Novomisle, W. A.; Ruggeri, R. B.; Tracey, W. R.; Hill, R. J. *Bioorg. Med. Chem. Lett.* **2001**, *11*, 803; (b) Pettersen, J. C.; Chouinard, L.; Kerlin, R. L.; Groom, S. N.; Botts, S.; Arezzo, J. C.; Boucher, M. A.; Frazier, D. E.; Buchholz, A. R. *Toxicol. Pathol.* **2008**, *36*, 608.
12. (a) *Affinity-Assay for the Human ERG Potassium Channel*; Greengrass, P.M.; Stewart, M.; Wood, C.M. PCT Patent Application WO 03/021271.; (b) Singleton, D. H.; Boyd, H.; Steidl-Nichols, J. V.; Deacon, M.; de Groot, M. J.; Price, D.; Nettleton, D. O.; Wallace, N. K.; Troutman, M. D.; Williams, C.; Boyd, J. G. *J. Med. Chem.* **2007**, *50*, 2931.
13. Davey, D. D. *J. Org. Chem.* **1987**, *52*, 4379.
14. (a) Miyazaki, M.; Dobrzyn, A.; Man, W. C.; Chu, K.; Sampath, H.; Kim, H. J.; Ntambi, J. M. *J. Biol. Chem.* **2004**, *279*, 25164; (b) Miyazaki, M.; Kim, Y. C.; Ntambi, J. M. *J. Lipid Res.* **2001**, *42*, 1018; (c) Flowers, M. T.; Ntambi, J. M. *BBA-Mol. Cell. Biol. L* **2009**, *1791*, 85.
15. Mar-Heyming, R.; Miyazaki, M.; Weissglas-Volkov, D.; Kolaitis, N. A.; Sadaat, N.; Plaisier, C.; Pajukanta, P.; Cantor, R. M.; de Bruin, T. W. A.; Ntambi, J. M.; Lusa, A. J. *Arterioscler. Thromb. Vasc. Biol.* **2008**, *28*, 1193.
16. TestDiet #5803.
17. Ramtohl, Y. K.; Black, C.; Chan, C.-C.; Crane, S.; Guay, J.; Guiral, S.; Huang, Z.; Oballa, R.; Xu, L.-J.; Zhang, L.; Li, C. S. *Bioorg. Med. Chem. Lett.* **2010**, *20*, 1593.